Assessment of Simulation Modelling and Real-Time Measurements for 3.15 and 17.28 kWp Solar Photovoltaic (PV) Systems in Malaysia

Banupriya Balasubramanian*‡, Azrul Mohd Ariffin*, Samer Husam Al-Zubaidi *,**

*Center for Renewable Energy (CRE), Universiti Tenaga Nasional (UNITEN), Jalan IKRAM – UNITEN, Kajang, Selangor, Malaysia

**M+W Group, San Diego, California, United States

(backiabanu@gmail.com, Azrula@uniten.edu.my, samer86h@yahoo.com)

‡Corresponding Author; Banupriya Balasubramanian, Center for Renewable Energy (CRE), Universiti Tenaga Nasional (UNITEN), Jalan IKRAM – UNITEN, Kajang, Selangor, Malaysia, Tel: +03-8921 2020, backiabanu@gmail.com

Received: 25.09.2016 Accepted: 28.11.2016

Abstract- The aim of this research work is to develop a portable simulation system that can measure ambient temperature (T_a) and solar irradiance (G) in real time, and then compute the energy that can be generated from a pre-defined PV system using these measurement data via a built-in graphic user interface (GUI). In constructing this system, a simulation modelling of PV output based on cell temperature and solar irradiance has been developed. The model was based on the first principles of representing a solar module with an equivalent circuit that takes into account the cell temperature, solar irradiance and all other parameters related to the cell. The accuracy of this simulation system was then being validated using the solar panel manufacturer's datasheet and also two PV systems that are available; 3.15 kWp solar PV rooftop system and 17.28 kWp solar PV carport system. Good agreements have been found between the simulated results and the measured field data. The developed simulation system can be potentially used in forecasting the power output generated by a solar module at a specific location without the need for actual installation.

Keywords Portable simulation system; Graphic user interface; UNITEN; Solar PV rooftop system; Simulation modelling; Cell temperature.

1. Introduction

PV array in a photovoltaic system is the crucial and most expensive part in producing electricity [1]. However the PV array performance depends on climatic, operating and design parameters such as ambient temperature, solar radiation intensity, cell temperature, overall heat loss coefficient, open-circuit voltage, short-circuit current, maximum power point voltage, maximum power point current and array area [2, 3]. The technical data provided by the manufacturers may not necessarily describe the performance of photovoltaic modules at a particular site because the climatic conditions can differ dramatically from the standard test conditions. This may lead to over or under estimation of energy production in real working conditions. Therefore, the knowledge on the characteristics of solar photovoltaic modules under real operating conditions is of great importance in determining their performance [4, 5].

Due to the above mentioned reasons, the demand on simulation scheme and operational technologies of photovoltaic systems and devices have also increased [6]. Modelling of photovoltaic cells could be beneficial in predicting the important characteristics of solar photovoltaic modules under real operating conditions. This paper utilizes the single diode model in the simulation modelling of PV cells with various solar module technologies incorporated. Influence of solar irradiation and ambient temperature to the performance of solar cells was simulated and analyzed. The developed model was then validated with manufacturer's technical data sheet and also with two installed solar PV systems at Universiti Tenaga Nasional (UNITEN).

2. Methodology

2.1. Modelling of Solar PV Output

The first task in developing the portable system to predict the energy that can be generated by a solar PV system is to come up with the simulation modelling. The model was based on the theories related to the circuit equivalent that can represent the principles working of a solar PV system. In simulating the output, the solar PV system needs to be defined first in the model. The definition includes the type of PV cell under study, its electrical characteristics, the number of panel used for the system, the configuration of these panels, so on and so forth. Once the PV system to be studied has been defined, the model will then proceed with utilizing the ambient temperature and solar irradiance measurements to simulate the solar PV output. The output simulated will be for a period of time as long as the ambient temperature and solar irradiance measurements are recorded.

2.1.1. Estimation of Cell Temperature Based on Ambient Temperature

Since the aim of the simulation tool is to compute the expected solar PV generation based on real-time ambient temperature and solar irradiance, it is important to choose the best estimation formula for the cell temperature. As explained as follows, that several formulae have been used by different researchers in establishing the relationship between the cell and ambient temperatures. Fig. 1 shows the plot of the simulated cell temperature based on the equations described below against the actual cell temperature measured by one of the installed solar PV systems at UNITEN for a period of five days of measurement data.

As reported in Ref [7-9],

$$T_c = T_a + \frac{NOCT - 20}{G_{NOCT}} G \tag{1}$$

where T_c is the cell temperature (°C), T_a is the corresponding ambient temperature (°C), NOCT is the nominal operating cell temperature (°C) and G is the irradiance received (W/m^2).

As reported in Ref [10],

$$T_c = T_a + 0.035G \tag{2}$$

where T_c is the cell temperature (°C), T_a is the corresponding ambient temperature (°C) and G is the irradiance received (W/m^2).

As reported in Ref [11],

$$T_c = T_a + \left(G \times \frac{\tau\alpha}{UL}\right) \times \left(1 - \frac{\mu}{\tau\alpha}\right), \quad \text{where } \frac{\tau\alpha}{UL} = \frac{T_{c,NOCT} - T_{a,NOCT}}{G_{1,NOCT}} \tag{3}$$

where τα is the absorptivity of the module. Absorptivity of a module is defined as the ratio of the total radiation absorbed by a module to the total amount of radiation striking the surface of a module. At least ninety percent of the radiation falling on a module should be absorbed. UL is the loss coefficient, $T_{c,NOCT}$ is the nominal operating cell temperature given in module specification data sheet, $T_{a,NOCT}$ is the ambient temperature for NOCT conditions (usually 20°C), $G_{1,NOCT}$ is the irradiance for NOCT conditions (usually 800 W/m^2) and μ is the efficiency of the PV cell.

As reported in Ref [12],

$$T_c = \frac{T_a + (T_{c,NOCT} - T_{a,NOCT})\left(\frac{G}{G_{1,NOCT}}\right)\left[1 - \frac{\eta_{STC}(1 - \alpha_p T_{c,STC})}{\tau\alpha}\right]}{1 + (T_{c,NOCT} - T_{a,NOCT})\left(\frac{G}{G_{1,NOCT}}\right)\left(\frac{\alpha_p \eta_{STC}}{\tau\alpha}\right)} \tag{4}$$

where η_{STC} is the efficiency under standard test conditions, α_p is the temperature coefficient of power and $T_{c,STC}$ is the cell temperature under standard test condition, typically 25°C.

As reported in Ref [13],

$$T_c = T_a + (219 + 832K_t) \times \frac{NOCT - 20}{G_{NOCT}} \tag{5}$$

where K_t is the monthly clearness index (range between 0.2 for a very overcast climate and 0.8 for a very sunny climate).

Ideally, it is best to estimate the simulated cell temperature as close as possible to the actual cell temperature measured by the PV system itself. As can be seen in Fig. 1, the accuracy for the equations used to estimate the cell temperature based on the ambient temperature measurements varies to different degrees, but it can be said that the equations presented in Ref [11], Ref [10] and Ref [7-9] give high accuracy in estimating the solar cell temperature so any of them can be used satisfactorily in simulating the solar PV output. For this research work, equation presented in Ref [7-9] has been chosen as it is deemed as not too simplistic in

nature but at the same time does not have too many parameters to assume. In simulating the cell temperature using this equation also, an error of ±5°C was also take into account, as suggested in Ref [14].

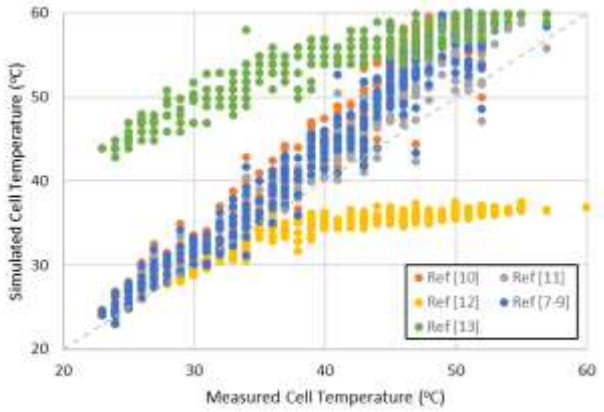

Fig. 1. Comparing the simulated cell temperature and actual cell temperature measured by the solar PV system installed at UNITEN.

2.1.2. Simulation of Current-Voltage and Power-Voltage Characteristics

The characteristics of solar PV cells can be represented using the concept of circuit equivalence. In this research work, a single diode with a series resistance model (shown by Fig. 2) was chosen because of its simplicity with less assumptions needed to be made for certain parameters, and also its ability to achieve accuracy as high as the more complex circuit representation of solar PV panel [15, 16].

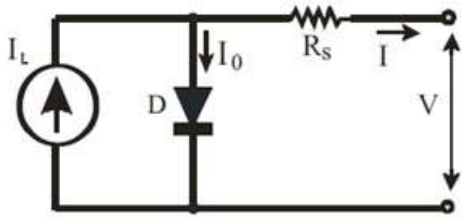

Fig. 2. Simple circuit representation used to simulate solar PV output [17].

The equations used to compute the PV output are explained as follows. I-V relationship of the solar cell with single-diode and series resistance is given as: [9, 18-21]

$$I = I_L - I_O = I_L - I_{OS}\left[\exp\left(q \times \frac{V + IR_S}{AkT_c}\right) - 1\right] \quad (6)$$

where I_L is the photo generated current, I_O is the diode current, I_{OS} is the reverse saturation current, q is the electronic charge (1.6 x 10^{-19} C), R_S is the resistance of the semiconductor, A is the cell ideality factor (1 for an ideal diode, varies between 1 and 2), k denotes the Boltzmann constant (1.38 x 10^{-23} J/K) and T_c is the cell temperature.

The photo generated current I_L is related to the short circuit current of the solar cell I_{SC} based on Eq. (7). The light induced current of the solar cell is dependent on the solar radiation G and also the cell temperature T_c of the solar cell [22-24].

$$I_L = [I_{SC} + \alpha(T_c - T_1)] \times \frac{G}{G_1} \quad (7)$$

where α is the temperature co-efficient of I_{SC}, T_1 is the reference temperature and G_1 is the reference irradiance (typically 1000 W/m^2). The reverse saturation current I_{OS} on the other hand, may be expressed as:

$$I_{OS} = I_{OS(T_1)} \times \left(\frac{T_c}{T_1}\right)^3 \times \exp\left[q \times \frac{E_g}{Ak}\left(\frac{1}{T_1} - \frac{1}{T_c}\right)\right] \quad (8)$$

where E_g is the energy or band gap and $I_{OS(T1)}$ is the reference saturation current. From the Eq. (8), it can be seen that the diode saturation current is dependent on temperature [22-23, 25-28]. The saturation current at reference temperature can be estimated using Eq. (9):

$$I_{OS(T_1)} = \frac{I_{SC(T_1)}}{\exp\left(q \times \frac{V_{OC(T_1)}}{N_S AkT_1}\right) - 1} \quad (9)$$

where $I_{SC(T1)}$ is short circuit current at reference temperature, $V_{OC(T1)}$ is open circuit voltage at reference temperature and N_S is the number of cells in series in a module.

The series resistance R_S value can be approximated by manipulating Eq. (6) by using the values for voltage, $V_{M(T1)}$ and current, $I_{M(T1)}$ at reference temperature that give maximum power output, as per stated in the manufacturer's datasheet. Manipulating this equation, the series resistance can be found using the following equation:

$$R_S = \frac{\frac{N_S AkT_1}{q} \times \ln\left(\frac{I_{SC(T_1)} - I_{M(T_1)}}{I_{OS(T_1)}} + 1\right) - V_{M(T_1)}}{I_{M(T_1)}} \quad (10)$$

The open circuit voltage V_{OC} is the voltage when current decreases to zero. In other words, all current generated by the solar cell flows through the diode and no power output will be generated. By rearranging Eq. (6) this open circuit voltage is given as:

$$V_{OC} = \frac{N_S AkT_c}{q} \times \ln\left(\frac{I_L}{I_{OS}} + 1\right) \quad (11)$$

Rearranging Eq. (6) also gives the voltage as a function of current:

$$V = \frac{N_S A k T_c}{q} \times \ln\left(\frac{I_L - I}{I_{OS}} + 1\right) - IR_S \qquad (12)$$

Throughout the I-V characteristic of a solar cell, the power output starts off from zero, reaches a maximum value, P_{MAX} and then decreases again to zero. The two points of zero power occur during the short circuit (V = 0) and open circuit (I = 0) conditions.

Using these equations, the variation of current as a function of voltage can therefore be determined. The current-voltage relationship for one panel differs from another panel depending on their electrical characteristics. Furthermore, this relationship is also greatly influenced by the cell temperature and solar irradiance that is incident upon the panel. From the current-voltage relationship simulated, the power-voltage relationship for a particular panel at a certain cell temperature and solar irradiance can be established by simply multiplying the current and voltage at each point. Fig. 3 illustrates the detailed mechanism of the simulation modelling used for this research work.

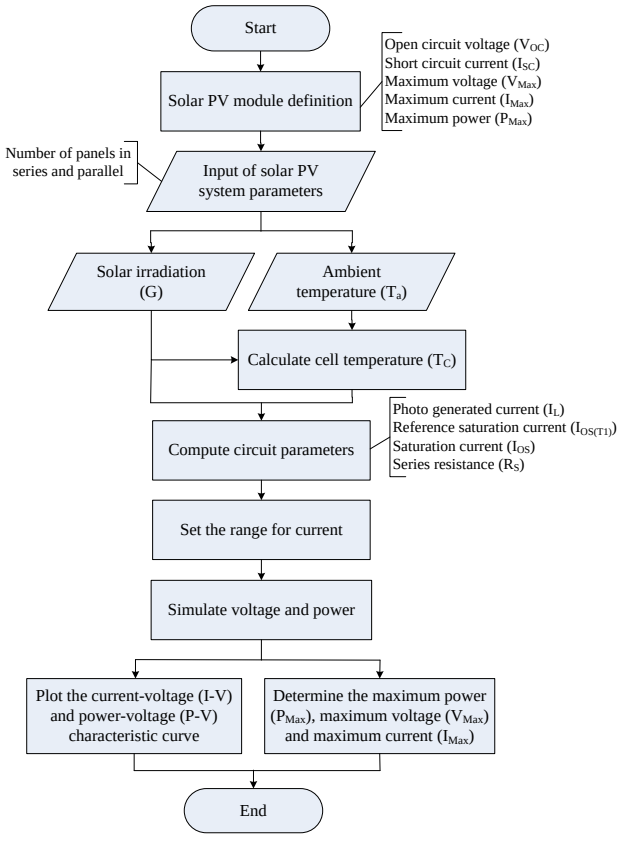

Fig. 3. Flowchart of simulation modelling of solar PV output using actual ambient temperature and solar irradiance measurements.

2.2. Portable Solar PV Simulation System

Using the theories relating to power output generation by solar PV, a portable system has been developed to predict the solar energy that can be generated using ambient temperature and solar insolation as inputs for a specific PV system. The system consists of two main parts: the first part is the system hardware which records the temperature and irradiation measurements, whereas the second part is the system software that uses the measurement data to simulate the output generation. The interfacing between the hardware setup and the software installed in a laptop can be done wirelessly or by using a cable. Fig. 4 illustrates the described portable solar PV simulation system.

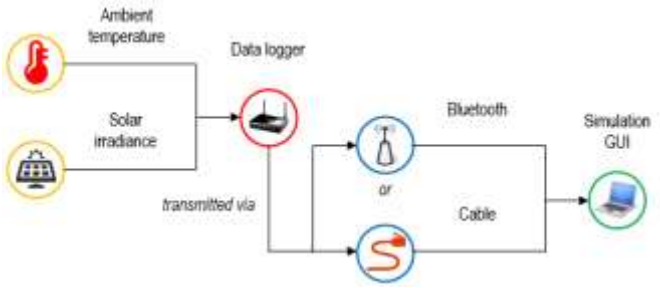

Fig. 4. Overall portable system developed to simulate solar PV system output based on real-time measurements.

SMA Sunny SensorBox and WebBox with Bluetooth Wireless Technology were used for this research work to measure the solar irradiation and ambient temperature directly and continuously. This system is equipped with a sensor kit (Sunny SensorBox) with integrated irradiation and temperature sensor which automatically captures data at a particular time and then transferred to a data logger (Sunny WebBox) using Bluetooth wireless interface. Solar irradiation and ambient temperature were recorded at intervals of every 5 or 15 minutes, and then the collected data was downloaded in the format of .CSV file. This allows the measurement of real-time irradiance and ambient temperature to be used as inputs for the solar PV output simulation using a laptop via built-in software. Fig. 5 shows the hardware configuration of the portable solar PV system.

Fig. 5. Portable solar measurement system and data logger.

A simulation software has been developed in Microsoft Visual Studio (.Net) platform to utilize the solar insolation and ambient temperature measurements recorded by the SMA Sunny WebBox, and then simulate the power output generated by a defined solar PV system. Fig. 6 shows an example of current-voltage and power-voltage characteristics obtained from the simulation modelling at standard testing condition (solar irradiance of 1000 W/m^2 and cell temperature of 25^{o}C) using the electrical characteristics of the panel used in one of the solar PV systems in UNITEN.

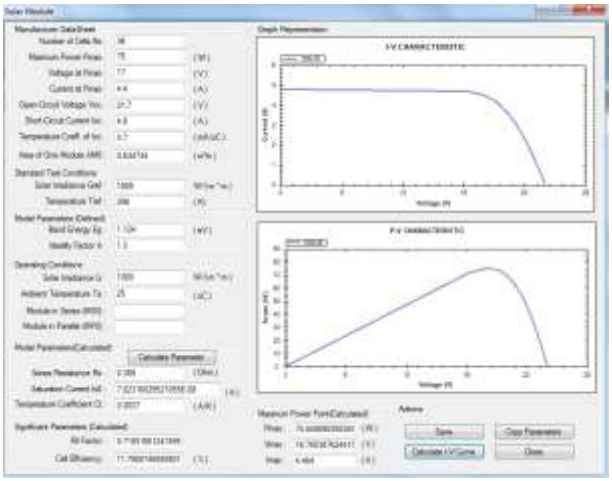

Fig. 6. Sample of current-voltage and power-voltage output plots at standard condition obtained from the simulation modelling.

2.3. Installed Solar PV system at UNITEN

In order to evaluate the performance of the developed portable solar PV simulation system, the simulation results obtained based on real-time ambient temperature and solar radiation will be compared with an actual solar PV system. The comparison between the simulation data and actual measurements will allow for the accuracy of the developed portable system to be determined. There are two solar PV systems at UNITEN that will be considered to achieve this objective.

2.3.1. 3.15 kWp Solar PV Rooftop System

The first system is a 3.15 kWp Building Integrated Photo-Voltaic (BIPV) system located at the rooftop of the BN building, College of Engineering (COE), UNITEN. Constructed in July 1998, the project was initiated by TNB Research Sdn Bhd (TNBR) with sponsorships from Malaysia Electricity Supply Industry Trust Account (MESITA) and Tenaga Nasional Berhad (TNB). This solar PV rooftop system is linked to the three phase electricity system of the building, and it was designed primarily for research studies of grid connected PV system [29].

The solar PV rooftop system is shown by Fig. 7. The system comprises forty two 75 Wp Siemens / Shell SP mono-crystalline modules configured in a 6 parallel by 7 series string installation. The system is also equipped with a grid-interactive inverter and PV meter. Solar irradiation, ambient temperature, cell temperature and the power produced by the PV system are recorded for every 15 minutes of time interval.

Table 1 outlines the electrical characteristics of the Siemens / Shell SP mono-crystalline module used in generating solar energy. This information is very important in order to simulate the expected output by this solar PV rooftop system as accurately as possible.

Fig. 7. The 3.15 kWp solar PV rooftop system.

2.3.2. 17.28 kWp Solar PV Carport System

Another system that will be referred to in evaluating the accuracy of the solar energy generation simulation results is the 17.28 kWp solar PV carport system. Located at the car park area of the Facility and Development Management Department (FDM), this system was originally constructed in 2012 to study the charging mechanism for electric vehicles by solar energy, and also to serve as sheds for the parked vehicles. The complete carport system is shown in Fig. 8.

Fig. 8. The 17.28 kWp solar PV carport system.

The car port PV system comprises of seventy two 240 Wp Q-Cells multi-crystalline modules configured in a 6 parallel by 12 series string combination installed. Each pair of the 12 module string configuration is connected to one inverter representing one phase. The electrical characteristics of the multi-crystalline modules used for this solar carport system is given in Table 1.

Table 1. Key specifications of chosen modules [30, 31].

Specification Parameter	SP 75 Wp Module	Q-Cells 240 Wp Module
Maximum Power Rating (P_{MAX})	75 W	240 W
Rated Current (I_{MPP})	4.4 A	8.15 A
Rated Voltage (V_{MPP})	17 V	29.37 V
Short Circuit Current (I_{SC})	4.8 A	8.72 A
Open Circuit Voltage (V_{OC})	21.7 V	37.14 V
Number of Cells in Series (N_S)	36	60
NOCT	45ºC	47ºC
Dimensions	1200 x 527 x 34 mm	1670 x 1000 x 50 mm

3. Results and Discussions / Simulation Results

3.1. Validation of Real-Time Measurement System

In order to ensure the developed portable solar PV simulation system works as it should be, it is first crucial to assess the accuracy of the ambient temperature (T_a) and solar irradiance (G) measured by the SMA Sunny SensorBox. The accuracy of these measurements may be determined by comparing them with the actual measurements recorded by one of the installed solar PV systems at UNITEN. In this case, the comparison was made against the ambient temperature and solar irradiance measurements recorded by the 17.28 kWp solar PV carport system. The correlation factor (k) was determined by evaluating the gradient of the linear trendline obtained from the scatter data plots. It can be safely assumed that the nearer the value of k to 1, the better the correlation between the two variables under study. Fig. 9 and 10 illustrate the comparison between the measured ambient temperature and solar radiance recorded by the Sunny Sensorbox and the aforementioned carport system respectively.

From Fig. 9, it can be seen that the ambient temperature measured by the Sensorbox has some degree of deviation from those recorded by the solar PV carport system, especially at high temperature. The correlation factor (k) between these two is 1.40. Thus it can be said that even though the ambient temperature recorded Sunny Sensorbox has a linear relationship with the temperature recorded by the carport system, the value may not be so accurate. The discrepancy between these two measurements may be attributed by a lot of factors such as the type and sensitivity of the temperature sensor used for each system, and also the placement of the sensors. Nevertheless, the more important thing is to determine the correlation factor of the simulated cell temperature (T_c), which is based on the measured ambient temperature, with the actual cell temperature recorded by the existing solar PV systems installed at UNITEN. This is because the simulated cell temperature would be one of the parameters that determine the output generated by a specific solar PV system. The correlation between the simulated and measured cell temperature is discussed in the next section.

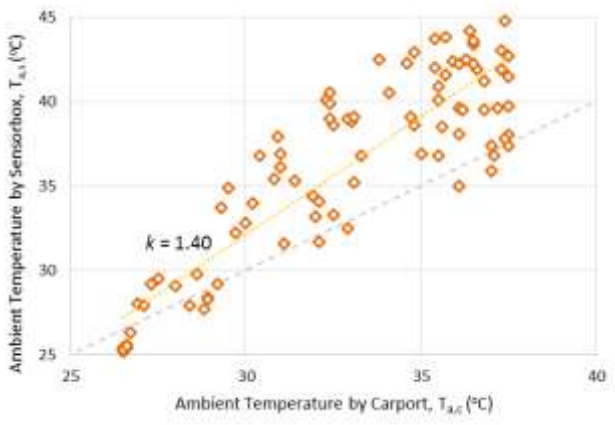

Fig. 9. Comparing the ambient temperature measured by SMA Sunny Sensorbox and the ambient temperature recorded by the solar PV carport system.

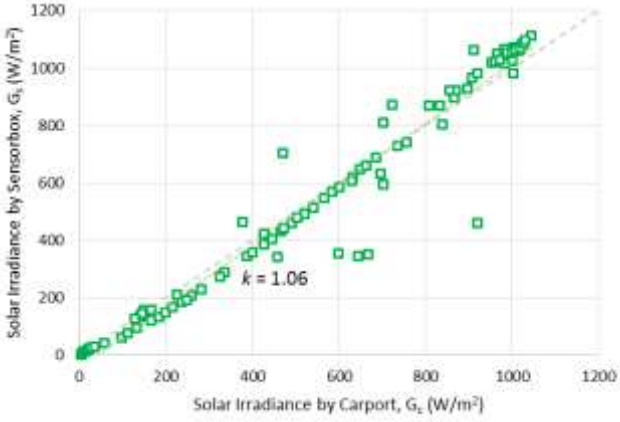

Fig. 10. Comparing the solar irradiance measured by SMA Sunny Sensorbox and the solar irradiance recorded by the solar PV carport system.

For solar irradiance on the other hand, it can be seen from Fig. 10 that there is a good agreement between the measurements obtained from the Sunny Sensorbox with the ones recorded by the carport system, with a correlation factor (k) of 1.06. This indicates that the solar irradiance measurement obtained from the Sensorbox can be used directly as one of the inputs for the portable solar PV simulation system because it can represent the actual irradiance incident upon a PV module with a high degree of accuracy.

3.2. Validation of Solar PV Simulation System

Using the ambient measurements as inputs, the accuracy of the simulated solar PV output can be assessed. In doing so, the accuracy of the simulated cell temperature (T_c) must be assessed first since it is based on the measured ambient temperature (T_a). Then using the simulated T_c and real-time solar irradiance G values, the solar PV outputs may be simulated. The accuracy of these simulation results will then be determined by comparing them with the actual values

obtained from several solar module manufacturers' datasheet and also from the output generated from the installed solar PV systems at UNITEN.

3.2.1. Comparing Simulated and Measured Cell Temperature

As discussed earlier, it has been suggested that the solar cell temperature (T_c) can be estimated based on the ambient temperature (T_a) and solar irradiance (G) using the equation given in Ref [7-9]. Taking the ambient temperature values obtained from the solar PV carport system as shown by Fig. 9 together with the solar irradiance measured, the corresponding cell temperature can therefore be computed. The comparison between the simulated and measured cell temperature for the 17.28 kWp solar PV carport system is shown in the following Fig. 11. In addition to this, comparison was also made for the simulated and measured T_c using measurements recorded by the 3.15 kWp solar PV rooftop system which was also installed at UNITEN. Fig. 12 shows the comparison between the simulated and measured T_c for this system.

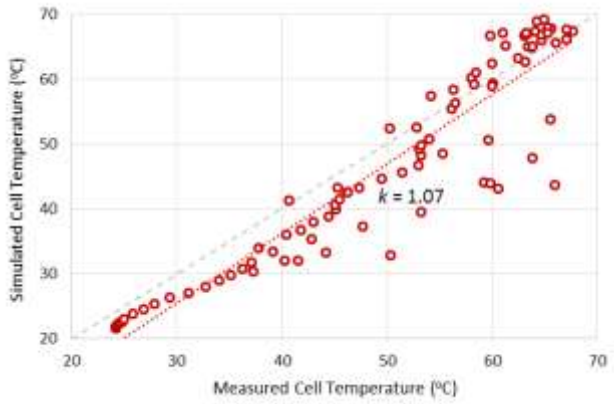

Fig. 11. Simulated and actual cell temperature for the solar PV carport system.

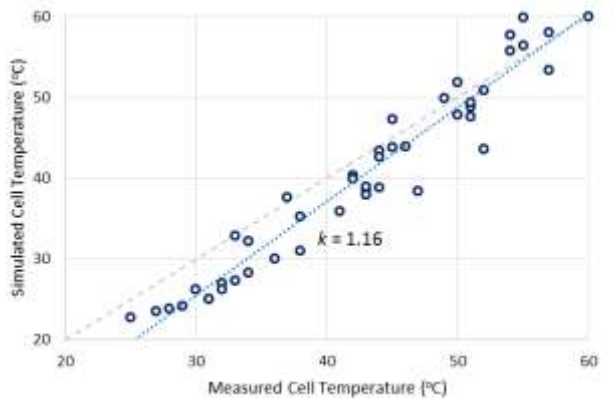

Fig. 12. Simulated and actual cell temperature for the solar PV rooftop system.

As can be seen from both figures, the correlation factor (k) between the simulated and measured T_c for both installed PV systems are much better (closer to 1) than the corresponding ambient temperature measurements shown in Fig. 9. This suggests that even though that the ambient temperature measured by the Sunny Sensorbox deviates prominently from the actual ambient temperature recorded by the solar PV system, its effects on the cell temperature can be considered as minimal. Thus the simulated cell temperature (T_c) based on the measured ambient temperature (T_a), together with the direct measurement of solar irradiance (G) from the developed system could reflect the actual condition responsible in determining the output of a solar PV system at a particular time.

3.2.2. Comparing Simulated PV Outputs with Manufacturer's Datasheet

After validating the accuracy of the inputs to be used for the simulation, the model was then verified by comparing the simulated outputs with solar cell manufacturer's datasheet. As explained earlier, the simulation was based on the single diode with a series resistance model for easy computation with less parameter assumptions. In comparing the simulated outputs with the manufacturer's datasheet, two types of solar module have been selected and they are:

- Siemens / Shell SP 75 Wp mono-crystalline silicon module
- Q-Cells 240 Wp multi-crystalline module

These solar modules are the ones that are currently used for the solar PV rooftop and carport systems installed at UNITEN. The electrical characteristics of the aforementioned solar modules can be referred from Table 1. It can be seen from Fig. 6, that simulation outputs exhibit common current-voltage (I-V) and power-voltage (P-V) characteristics of a solar panel.

The effects of varying solar cell temperature (T_c) and solar irradiance (G) on I-V and P-V characteristics were also investigated for both types of solar module. Influence of cell temperature and solar irradiance on the simulation outputs were studied. From the outputs, it was observed that the variation in cell temperature and solar irradiance would affect both I-V and P-V characteristics of a particular solar module. As cell temperature increases, the module's open circuit voltage (V_{oc}) decreases whereas its short circuit current (I_{sc}) increases albeit at a relatively much smaller rate in comparison with the reduction in the open circuit voltage. Both open circuit voltage and short circuit current however, increase with the increase of solar irradiance.

The maximum power a solar module can generate is also affected by the cell temperature and solar irradiance variation. It was found from the simulation that the maximum power decreases with the increase of cell temperature. Thus there is an inverse relationship between the maximum power generated by any solar module with the cell temperature.

Table 2. Comparison of rated maximum power, current and voltage between values reported in manufacturer's datasheet with the simulated data.

Parameter	Siemens / Shell SP 75 Wp			Q-Cells 240 Wp		
	Claimed Value	Simulated Value	Difference	Claimed Value	Simulated Value	Difference
Rated Power (W)	75	74.84	0.21%	240	239.39	0.25%
Rated Current (A)	4.4	4.46	1.36%	8.15	8.11	0.49%
Rated Voltage (V)	17	16.77	1.35%	29.37	29.52	0.51%

On the other hand, the power generated increases with the solar irradiance incident upon a solar module. Thus it can be concluded that the maximum power that can be produced by a solar module depends very much on its cell temperature and the solar irradiance at any particular time, provided no form of degradation is experienced by the module.

It was observed that the simulated I-V and P-V characteristics follows the typical output of any solar PV module. This suggests that the simulation modelling works as it should be and thus can be used to predict the PV power output at any particular cell temperature and solar irradiance. The maximum power output was then compared against the manufacturer's claimed output at Standard Test Conditions (STC), with cell temperature of 25°C and solar irradiance of 1000 W/m^2 in order to assess the simulation accuracy. Table 2 outlines the comparison between the manufacturer's rated value and simulated data for maximum power, together with its corresponding voltage and current under STC.

From Table 2, it can be seen that there is a considerably good agreement between the simulated outputs with the values claimed by Siemens / Shell SP and Q-Cells for their modules operating at STC. The percentage difference between them for the rated power, current and voltage is less than 1.4%, with the maximum power having an even better percentage as low as 0.21%. This indicates that the simulation model has a remarkable accuracy in predicting the solar PV output at any particular cell temperature and solar irradiance. Nevertheless, one could also argue that the model works for simulating the output for a solar module only, not necessarily the output of a complete PV system. Thus the next section will discuss the comparison between the simulation data with the actual output generated by the two installed solar PV systems at UNITEN.

3.2.3. Comparing Simulated PV Power with Installed Systems

With an accuracy of around 99% in simulating power output at STC, the model was then being tested against the actual output generated by the 3.15 kWp solar PV rooftop system and 17.28 kWp solar PV carport system. As mentioned earlier, the cell temperature (T_c) was first estimated based on the ambient temperature (T_a) measured by the system hardware. Using the estimated cell temperature and solar irradiance (G) for a specific point of time, the power output (P) was then simulated for a particular solar PV system. The developed simulation software allows for a PV system to be defined based on the type of solar module used, the number of modules used and their connection configuration for that system. This would then enable a direct comparison between the simulated output and actual power measured by the two installed solar PV systems.

Fig. 13 shows the simulated and measured power as a function of time obtained from the solar PV rooftop system for one day. Comparing the two graphs, it can be seen that the measured solar power is significantly lower (by approximately 30%) than the expected power to be produced by this system. Similar observation was also found for several other days from this same system.

Upon further investigation, the difference between these simulated and measured power could be attributed due to the age of the system. The solar PV rooftop system was commissioned and constructed in 1998 so it is appropriate to expect that the panels and the system would have undergone some form of degradation after more than 10 years of service. Table 3 outlines some possible form of degradation that this system may have experienced together with its approximated derating factor. The total derating factor was obtained by multiplying each of the individual derating factor based on the type of degradation.

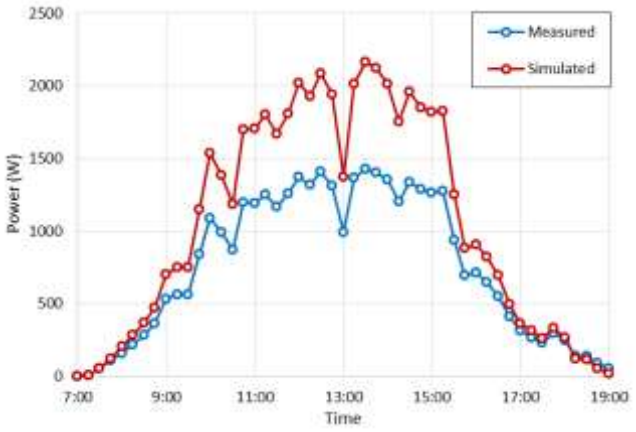

Fig. 13. Comparison of daily simulated and measured power obtained for 3.15 kWp solar PV rooftop system.

Table 3. Possible derating factors responsible for reduced power output.

Parameter / Factor	Value
Cable loss factor – f_{cable_loss} [32]	0.968
Dirt and dust – f_{dirt} [32]	0.97
Manufacturer's tolerance - f_{mm} [32]	0.95
Temperature – f_{temp_pmp} [33, 34]	0.86
Installation criteria [32]	0.98
Inverter efficiency - η_{inv} [35, 36]	0.943
PV to the inverter efficiency - η_{PV_inv} [33-36]	0.98
Overall Derating Factor	0.69

Taking into account the approximated overall derating factor of 0.69, the simulated power was then reduced to 69% of its initial value. It can be seen clearly now from Fig. 14 that the new simulated power is consistent with the actual power measurement. The correlation factor (k) also improves from 1.51 to 1.04 when the derating factor taken into consideration as shown by Fig. 15. This indicates that there is high possibility that the difference between the simulated and measured power observed for the solar PV rooftop system could be due to its old age. To validate this hypothesis further, a comparison was made between the simulated and measured output from the other solar PV system installed at UNITEN.

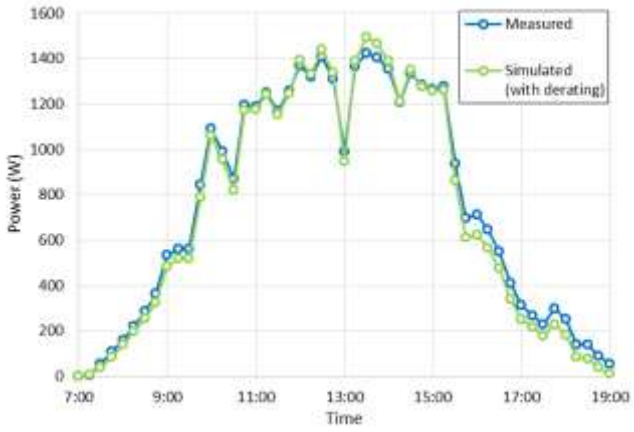

Fig. 14. Simulated (with derating factor) and measured power data for 3.15 kWp solar PV rooftop system.

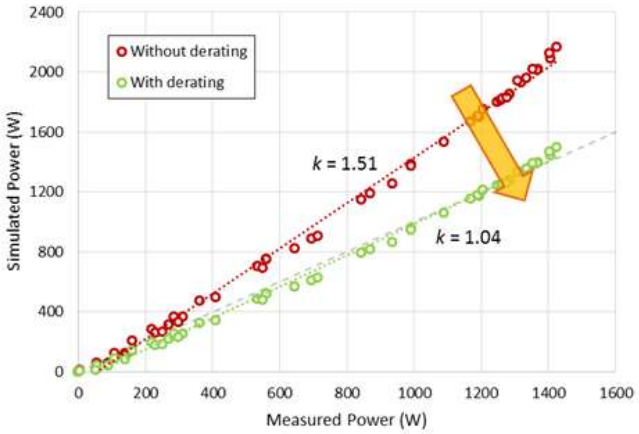

Fig. 15. Comparing the correlation between simulated and measured power under the influence of derating factor.

The solar PV carport system was constructed in 2012, which makes the system relatively newer compared to the rooftop system. With the real-time cell temperature and solar irradiance as inputs, the power output was simulated and then compared with the actual measurement obtained from the same system, as can be seen from Fig. 16. It was observed that there is smaller discrepancy between the simulated and the measured power for the solar PV carport system as compared to the rooftop system. This suggests that the age of the solar PV system plays a crucial part in determining the actual power produced by the system. It can be expected that the older a solar PV system is, the less power it can generate due to degradation of the system. Fig. 17 shows the degree of correlation between the simulated and measured power for the solar PV carport system. It was found that the correlation factor (k) of 1.11 for this system is still better as compared to the solar PV rooftop system with k = 1.51.

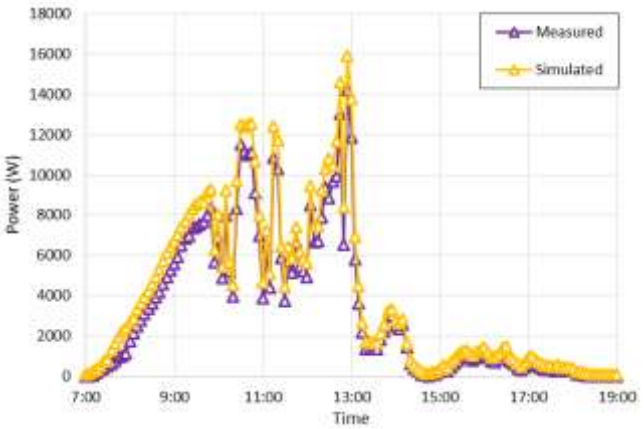

Fig. 16. Comparison of daily simulated and measured power obtained for 17.28 kWp solar PV carport system.

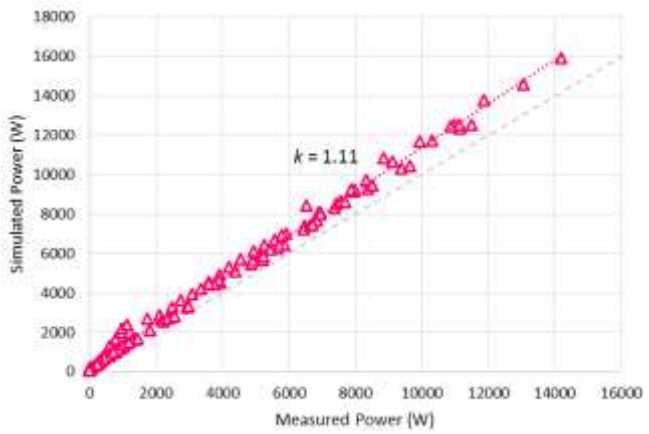

Fig. 17. Correlation between simulated and actual measured power for the solar PV carport system.

4. Conclusion

A portable simulation system for determining the solar power output based on real-time ambient temperature and solar irradiation measurements has been developed. The real-time ambient measurements from the developed portable solar PV simulation systems were compared and validated with those obtained from existing PV systems to deduce that any variance would be minimal. The two solar PV systems referred to for this study were the 3.15 kWp solar PV rooftop system and the 17.28 kWp solar PV carport system. The developed solar PV simulation system was then being tested and its simulated data verified using the existing PV systems. The computed solar PV cell temperature based on ambient temperature was compared with the actual cell temperature measured by the existing solar PV systems. Comparing the computed cell temperature with the actual one had shown that the equation chosen to estimate the cell temperature based on the measured ambient temperature was accurate enough to be used for the simulation of solar PV output. By using this approximation and the actual solar radiation measurement, the solar PV output was simulated using the electrical characteristics and configuration of the two aforementioned systems. It was found that the simulation of power output has a very good agreement with the solar PV carport system output, but the same cannot be said for the rooftop system. The difference between the simulated and measured power for this system was quite noticeable. Upon further investigation however, it was found out that the rooftop system had been commissioned for quite a number of years already and this could affect the performance of the solar panels. When the de-rating factor due to this was taken into account, the simulation data was found to be consistent with the measurement data from the solar PV system. Thus it can be deduced that the developed portable system is capable to simulate power output with great accuracy based on real ambient temperature and solar irradiance measurements.

Acknowledgements

The authors would like to acknowledge the financial assistance of Ministry of Higher Education (MOHE), Malaysia under the ERGS scheme for providing scholarships for this study.

References

[1] Arati Kane, and Dr.Vishal Verma, "Performance Enhancement of Building Integrated Photovoltaic Module using Thermoelectric Cooling", *International Journal of Renewable Energy Research*, vol. 3, pp. 320-324, April 2013.

[2] F. Sarhaddi, S. Farahat, H. Ajam, and A. Behzadmehr, "Exergetic Performance Evaluation of a Solar Photovoltaic (PV) Array", *Australian Journal of Basic and Applied Sciences*, vol. 4, pp. 502-519, March 2010.

[3] Mukesh Kumar Gupta, and Rohit Jain, "MPPT Simulation with DC Submersible Solar Pump using Output Sensing Direct Control Method and Cuk Converter", *International Journal of Renewable Energy Research*, vol. 3, pp. 186-191, March 2013.

[4] A. Ibrahim, M. R. I. Ramadan, A. A. El-Sebaii, and S. M. El-Broullesy, "Annual Performance of Solar Modules with Tilting Angle Facing South and Sun Tracking in Tanta, Egypt", *International Journal of Renewable Energy Research*, vol. 1, pp. 26-40, May 2011.

[5] Rustu Eke, and Sener Oktik, "Seasonal Variation of Internal Parameters of Amorphous Silicon (a-Si) Thin Film Photovoltaic Modules", *International Journal of Renewable Energy Research*, vol. 2, pp. 549-555, August 2012.

[6] VandanaKhanna, Bijoy Kishore Das, and Dinesh Bisht, "MATLAB/SIMELECTRONICS Models Based Study of Solar Cells", *International Journal of Renewable Energy Research*, vol. 3, pp. 30-34, December 2012.

[7] R. G. Ross, and M. I. Smokler, "Electricity from photovoltaic solar cells: Flat-Plate Solar Array Project final report. Volume VI: Engineering sciences and reliability", *JPL Publication*, pp. 86-31, October 1986.

[8] A. Ghouari, Ch. Hamouda, A. Chaghi, and M. Chahdi, "Data monitoring and performance analysis of a 1.6kWp grid connected PV system in Algeria", *International Journal of Renewable Energy Research*, vol. 6, pp. 34-42, December 2015.

[9] Sadok Mohammed, Benyoucef Boumediene, and Benmedjahed Miloud, "Assessment of PV Modules Degradation based on Performances and Visual Inspection in Algerian Sahara", *International Journal of Renewable Energy Research*, vol. 6, pp. 106-116, January 2016.

[10] Luis Castaner, and Santiago Silvestre, Modelling Photovoltaic Systems Using PSpice, England: John Wiley & Sons Ltd, 2002.

[11] Raam Perumal, "Loss Due to Ambient Temperature", *PVSyst Manual*, 2011.

[12] Marilyn Walker, "How HOMER Calculates the PV Cell Temperature?" Retrieved from http://support.homerenergy.com/index.php?/Knowledgebase/Article/View/489/0/10487---how-homer-calculates-the-pv-cell-temperature, 2012. [Accessed: Jul. 15, 2014].

[13] Suresh A/L Thanakodi, "Modeling and simulation of grid connected photovoltaic system using Matlab / Simulink", Master's thesis, Universiti Teknologi Malaysia, Skudai, Johor, Malaysia, November 2009.

[14] PVEducation, "Nominal Operating Cell Temperature", [Online] 2013. Available from: http://pveducation.org/. [Accessed: Nov. 09, 2013].

[15] Carrero, J. Amador, and S. Arnaltes, "A Single Procedure for Helping PV Designers to Select Silicon PV Module and Evaluate the Loss Resistances" *Renewable Energy*, vol. 32, pp. 2579-2589, December 2007.

[16] Andreas Wagner, "Peak-Power and Internal Series Resistance Measurement under Natural Ambient Conditions", *EuroSun Copenhagen*, June, 2000.

[17] Altas I. H., and Sharaf A. M, "A Photovoltaic Array Simulation Model for Matlab-Simulink GUI Environment", *International Conference on Clean Electrical Power (ICCEP '07)*, pp. 341-345, May 2007.

[18] Ramos Hernanz J. A., Campayo Martin J. J., Zamora Belver I., Larranaga Lesaka J., Zulueta Guerrero E., and Puelles Perez E, "Modelling of Photovoltaic Module", *International Conference on Renewable Energies and Power Quality (ICREPQ'10)*, March 2010.

[19] J. A. Gow, and C. D. Manning, "Development of a photovoltaic array model for use in power-electronics simulation studies", *IEE Proceedings-Electric Power Applications*, vol. 146, pp. 193-200, 1999.

[20] A. Ibrahim, and A. A. El-Amin, "Temperature Effect on the Performance of of n-Type uc -Si Film Grown by Linear Facing Target Sputtering for Thin Film Silicon Photovoltaic Devices", *International Journal of Renewable Energy Research*, vol. 2, pp. 160-165, February 2012.

[21] André Coelho, and Rui Castro, "Sun Tracking PV Power Plants: Experimental Validation of Irradiance and Power Output Prediction Models", *International Journal of Renewable Energy Research*, vol. 2, pp. 23-32, October 2011.

[22] W. De Soto, S. A. Klein, and W. A. Beckman, "Improvement and validation of a model for photovoltaic array performance", *Solar Energy*, vol. 80, pp. 78-88, January 2006.

[23] Q. Kou, S. A. Klein, and W. A. Beckman, "A method for estimating the long-term performance of direct-coupled PV pumping systems", *Solar Energy*, vol. 64, pp. 33-40, September 1998.

[24] A. Driesse, S. Harrison, and P. Jain, "Evaluating the effectiveness of maximum power point tracking methods in photovoltaic power systems using array performance models", *IEEE Power Electronics Specialists Conference (PESC)*, pp. 145-151, June 2007.

[25] R. A. Messenger, and J. Ventre, Photovoltaic systems engineering, CRC Press, 2004.

[26] F. Nakanishi, T. Ikegami, K. Ebihara, S. Kuriyama, and Y. Shiota, "Modeling and operation of a 10 kW photovoltaic power generator using equivalent electric circuit method", *Conference Record of 28th IEEE Photovoltaic Specialists Conference*, pp. 1703-1706, September 2000.

[27] J. Crispim, M. Carreira, and R. Castro, "Validation of photovoltaic electrical models against manufacturers data and experimental results", *International Conference on Power Engineering, Energy and Electrical Drives (POWERENG)*, pp. 556-561, April 2007.

[28] K. H. Hussein, I. Muta, T. Hoshino, and M. Osakada, "Maximum photovoltaic power tracking: an algorithm for rapidly changing atmospheric conditions", *IEE Proceedings-Generation, Transmission and Distribution*, pp. 59-64, January 1995.

[29] Ahmad Hadri Haris, "Grid-connected and Building Integrated Photovoltaic: Application Status & Prospect for Malaysia", MBIPV Project, PTM (Malaysia Energy Centre), 2006.

[30] Siemens / Shell SP-75 Module Technical Datasheet. Retrieved from http://www.solardirect.com/PDF/SolarElectric/sp75.pdf

[31] Q-Cells 240 Wp Module Technical Datasheet. Retrieved from http://www.q-cells.com/uploads/tx_abdownloads/files/Q-Cells_QBASE-G2_Data_sheet_2011-06_Rev02.pdf

[32] Hedzlin Zainuddin., Sulaiman Shaari., Ahmad Maliki Omar., and Shahril Irwan Sulaiman, "Power Prediction for Grid-Connected Photovoltaic System in Malaysia", *3rd International Symposium & Exhibition in Sustainable Energy & Environment*, pp. 110-113, August 2011.

[33] Ahmad, V. Tan, W. N. Chen, and D. Ruoss, "11.88 kWp BIPV System Installation at Putrajaya Perdana Berhad HQ, P16, Putrajaya", *Malaysia Building Integrated Photovoltaic (MBIPV) Project*, 2007. Retrieved from http://www.mbipv.net.my/dload/MBIPV%20Reports/C2/Putrajaya%20Perdana%20Bhd.pdf

[34] Ahmad, V. Tan, W. N. Chen, and D. Ruoss, "4.2 kWp BIPV System Installation at No 96, Lot 5650, Lorong Indah 2, Taman Perkota, Bukit Sebukor Melaka", *Malaysia Building Integrated Photovoltaic (MBIPV) Project*, 2007. Retrieved from http://www.mbipv.net.my/dload/MBIPV%20Reports/C2/Bt%20Sebukor%20Melaka.pdf

[35] Ahmad, V. Tan, W. N. Chen, and D. Ruoss, "4.0 kWp BIPV System Installation at Lot 488, Jalan Khaya, Country Heights Damansara, Petaling Jaya", *Malaysia Building Integrated Photovoltaic (MBIPV) Project*, 2007. Retrieved from http://www.mbipv.net.my/dload/MBIPV%20Reports/C2/Damansara.pdf

[36] Ahmad, V. Tan, W. N. Chen, and D. Ruoss, "9.9 kWp BIPV System Installation at Damansara Utama Shoplots, Damansara Utama", *Malaysia Building Integrated Photovoltaic (MBIPV) Project*, 2007. Mmm Retrieved from http://www.mbipv.net.my/dload/MBIPV%20Reports/C2/Damansara%20Utama%20shoplots.pdf